

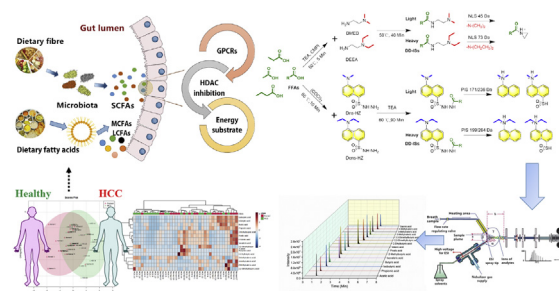
Integrated LC-MS metabolomics with dual derivatization for quantification of FFAs in fecal samples of hepatocellular carcinoma patients

Jiangang Zhang^{1,‡}, Shuai Yang^{1,2,‡}, Jingchun Wang¹, Yanquan Xu¹, Huakan Zhao^{3,4}, Juan Lei^{3,4}, Yu Zhou^{3,4}, Yu Chen^{3,4}, Lei Wu^{3,4}, Mingyue Zhou^{3,4}, Yan Li^{3,*}, and Yongsheng Li^{1,3,4,*}

¹Clinical Medicine Research Center, Xinqiao Hospital and ²Department of Pathology, the 958th Hospital, Southwest Hospital, Army Medical University, Chongqing, China; and ³Department of Medical Oncology and ⁴Chongqing Key Laboratory for Intelligent Oncology in Breast Cancer, Chongqing University Cancer Hospital, Chongqing, China

Abstract FFAs display pleiotropic functions in human diseases. Short-chain FFAs (SCFAs), medium-chain FFAs, and long-chain FFAs are derived from different origins, and precise quantification of these FFAs is critical for revealing their roles in biological processes. However, accessing stable isotope-labeled internal standards is difficult, and different chain lengths of FFAs challenge the chromatographic coverage. Here, we developed a metabolomics strategy to analyze FFAs based on isotope-free LC-MS-multiple reaction monitoring integrated with dual derivatization. Samples and dual derivatization internal standards were synthesized using 2-dimethylaminoethylamine or dansyl hydrazine as a “light” label and *N,N*-diethyl ethylene diamine or *N,N*-diethyldansulfonyl hydrazide as a “heavy” label under mild and efficient reaction conditions. General multiple reaction monitoring parameters were designed to analyze these FFAs. The limit of detection of SCFAs varied from 0.5 to 3 nM. Furthermore, we show that this approach exhibits good linearity ($R^2 = 0.99374\text{--}0.99929$), there is no serious substrate interference, and no quench steps are required, confirming the feasibility and reliability of the method. Using this method, we successfully quantified 15 types of SCFAs in fecal samples from hepatocellular carcinoma patients and healthy individuals; among these, propionate, butyrate, isobutyrate, and 2-methylbutyrate were significantly decreased in the hepatocellular carcinoma group compared with the healthy control group. These results indicate that the integrated LC-MS metabolomics with isotope-free and dual derivatization is an efficient approach for quantifying FFAs, which may be useful for identifying lipid biomarkers of cancer.

Supplementary key words FFAs • short-chain FFAs • LC-MS • isotope-free • derivatization • 2-dimethylaminoethylamine • dansyl hydrazine • *N,N*-diethyl ethylene diamine • *N,N*-diethyldansulfonyl hydrazide • hepatocellular carcinoma



FFAs are essential components of cell membrane and act as energy substrates for cells (1–3). By binding G protein-coupled receptors, they exert pleiotropic functions in signaling transduction pathways from cellular compartmentation to tissue response (2, 4, 5). Through histone acetylation, malonylation, butylation, and palmitoylation, FFAs function as metabolite substrates that epigenetically orchestrate the crosstalk between the gut microbiota and tumorigenesis (6–8). Considering their key functions of FFAs in the aforementioned processes, it is necessary to develop a comprehensive method for profiling FFAs in biosamples.

Based on their chain length, FFAs are classified as short-chain FFAs (SCFAs; ≤6 carbons), medium-chain FFAs (MCFAs; 6–12 carbons), and long-chain FFAs (LCFAs; more than 12 carbons). Owing to their volatility and thermal stability, the development of FFA analytical methodologies is traditionally based on GC-MS (9). However, dilemma such as high-energy, electron impact ionization, and low vapor pressure prevent the precise analysis of FFAs. LC-MS with flexible separation and soft ionization technique is thus increasingly gaining attention for FFA quantification (10, 11). Stable isotope-labeled chemical derivatization (CD) combined with LC-MS is evidenced as an effective tool for revolving low ionization efficiency of FFAs per se in the negative ion mode and lack of diagnostic fragments

[‡]These authors contributed equally to this work.

*For correspondence: Yongsheng Li, lys@cqu.edu.cn; Yan Li, pipili@sina.com.

for constructing multiple reaction monitoring (MRM) ion pairs (10, 12). For instance, Borchers *et al.* (13) used 3-nitrophenylhydrazine and its $^{13}\text{C}_6$ analogue to mark fecal SCFAs by LC-MS/MS in patients with type 2 diabetes. Chan *et al.* (14) developed a method for quantitatively measuring SCFAs in healthy infant stool samples derivatized with ^{12}C - and ^{13}C -labeled aniline. Feng *et al.* (15) applied 2-dimethylaminoethylamine (DMED) and d_4 -DMED to label the arachidonic acid metabolome in rat tissues. Zhao and Li (16) reported ^{13}C - and ^{12}C -dansyl hydrazine (Dns-Hz) labeling of the carboxyl submetabolome, and a total of 2,266 peak pairs or metabolites were detected. Xu *et al.* (17) displayed two structural analogues, 5-dimethylamino-naphthalene-1-sulfonyl piperazine (Dns-PP) and diethylamino-naphthalene-1-sulfonyl piperazine (Dens-PP) for quantifying FFAs. These studies generally adopt the reactivity of carboxyl moieties with amines by converting FFAs to a class of acylamides, by which the ionization efficiency of the derivatives is abundantly amplified. Nevertheless, owing to the cost and availability of stable isotope reagents, the easy-to-use and comprehensive isotope-free based CD methods for specific quantification of FFAs remain sparse.

Here, we illustrate an integrated isotope-free method with dual derivatization strategy using LC-MS metabolomics to quantify FFAs. By manipulating a pool of synthesized or commercially available reagents, light mass structural analogues (DMED or Dns-Hz) were

employed to label samples, whereas heavy mass structural analogues (*N,N*-diethyl ethylene diamine [DEEA] or *N,N*-diethyl dansulfonyl hydrazide [Dens-HZ]) tagged standard mixtures were devised as dual derivatization internal standards (DD-ISs). In addition, DMED/DEEA for dual derivatization of SCFAs was demonstrated and validated by quantifying fecal SCFAs from hepatocellular carcinoma (HCC) patients and healthy individuals.

MATERIALS AND METHODS

Reagents and lipid standards

Standard compounds of FFAs (listed in Tables 1 and 2), Dns-Hz, and acetic acid- $^{13}\text{C}_2$ sodium salt ($\text{C}_2:0\text{-}^{13}\text{C}_2$, total number of carbon atoms: degree of unsaturation) were all purchased from Sigma-Aldrich (St. Louis, MO). HPLC-grade acetonitrile (ACN), methanol, dichloromethane (DCM), and isopropanol (IPA) were obtained from Honeywell B&J (Moorestown, NJ). Deionized water was obtained from a Millipore Milli-Q purification system (Bedford, MA, UK). DMED and its analogue DEEA, *N,N*-dimethylformamide, triethylamine (TEA), oxalyl chloride (2 M in DCM), trichloromethane (TCM), and 2-chloro-1-methylpyridinium iodide (CMPi) were purchased from InoChem Tech Co, Ltd (Beijing, China). We used oxalyl chloride in a fume hood, while wearing the complete personal protective equipment (protective gloves, goggles, and clothing). In addition, the bottles were tightly sealed and stored in a cool and dry place to prevent contact with moisture. Propionic acid- d_5 ($\text{C}_3:0\text{-d}_5$) and butyric acid- d_7 ($\text{C}_4:0\text{-d}_7$) were purchased from Cambridge Isotope

TABLE 1. SCFAs analyzed by the method and compound-specific MS parameters

Q1 Mass (Da)	Q3 Mass (Da)	Dwell Time (s)	Analyte	DP (V)	EP (V)	CE (V)	CXP (V)
131.0	86.1	30	Acetic acid-DMED	27.0	3.1	17.0	21.0
159.0	86.0	30	Acetic acid-DEEA	44.3	6.0	20.7	9.8
145.1	100.0	30	Propionic acid-DMED	30.0	6.0	17.0	16.0
173.1	100.0	30	Propionic acid-DEEA	36.3	6.3	20.7	12.0
159.3	114.2	30	Isobutyric acid-DMED	23.8	6.0	17.0	13.0
187.1	114.1	30	Isobutyric acid-DEEA	47.5	5.7	19.0	6.0
159.1	114.1	30	<i>n</i> -Butyric acid-DMED	40.0	10.0	20.0	13.0
187.1	114.1	30	<i>n</i> -Butyric acid-DEEA	52.0	9.6	32.2	19.0
173.0	128.0	30	<i>n</i> -Valeric acid-DMED	22.0	6.0	18.4	13.0
201.1	128.2	30	<i>n</i> -Valeric acid-DEEA	60.0	8.0	27.0	12.0
173.2	128.1	30	Isovaleric acid-DMED	40.0	10.0	20.0	13.0
201.0	128.1	30	Isovaleric acid-DEEA	56.0	11.0	29.2	15.0
173.1	128.0	30	2-Methylbutyric acid-DMED	40.0	10.0	20.0	13.0
201.2	128.1	30	2-Methylbutyric acid-DEEA	35.7	8.3	18.8	15.0
187.1	142.1	30	2-Methylvaleric acid-DMED	40.0	10.0	20.0	13.0
215.0	142.1	30	2-Methylvaleric acid-DEEA	52.0	9.6	32.2	19.0
187.0	142.0	30	3-Methylvaleric acid-DMED	30.0	5.0	20.0	17.0
215.3	142.0	30	3-Methylvaleric acid-DEEA	47.5	8.2	22.9	16.0
187.1	142.0	30	4-Methylvaleric acid-DMED	40.0	10.0	20.0	13.0
215.1	142.2	30	4-Methylvaleric acid-DEEA	56.0	11.0	29.2	15.0
173.1	128.2	30	Pivalic acid-DMED	40.0	10.0	20.0	13.0
201.1	128.1	30	Pivalic acid-DEEA	56.0	7.0	30.6	17.0
187.1	142.1	30	2-Ethylbutyric acid-DMED	40.0	10.0	20.0	13.0
215.1	142.1	30	2-Ethylbutyric acid-DEEA	52.0	9.6	32.2	19.0
187.2	142.0	30	2,2-Dimethylbutyric acid-DMED	40.0	10.0	20.0	13.0
215.1	142.1	30	2,2-Dimethylbutyric acid-DEEA	60.0	8.0	27.0	12.0
187.2	142.0	30	3,3-Dimethylbutyric acid-DMED	40.0	10.0	20.0	13.0
215.1	142.0	30	3,3-Dimethylbutyric acid-DEEA	56.0	11.0	29.2	15.0
187.0	142.0	30	Hexanoic acid-DMED	40.0	10.0	20.0	13.0
215.0	142.0	30	Hexanoic acid-DEEA	56.0	7.0	30.6	17.0

CE, collision energy; CXP, collision cell exit potential; DP, declustering potential; EP, entrance potential.

TABLE 2. Sensitivity and linearity of LC-MS MRM assay

No.	Analyte	LOD (nM)	LOQ (nM)	Regression Line	R ²	Linear Range (nM)	Inter CV (%)	Intra CV (%)
1	Acetic acid	0.5	1.5	$y = 1.13938e^{-4}x + 0.01727$	0.99842	12–6,250	6.1	8.0
2	Propionic acid	1.5	5.0	$y = 1.91767e^{-4}x + 0.00564$	0.99846	10–12,500	5.1	6.4
3	Isobutyric acid	1.5	4.0	$y = 2.97287e^{-4}x + 0.01146$	0.99848	5–6,250	1.4	5.4
4	<i>n</i> -Butyric acid	0.5	2.0	$y = 4.35691e^{-5}x + 0.01852$	0.99436	5–25,000	5.2	5.0
5	<i>n</i> -Valeric acid	0.5	1.5	$y = 1.46422e^{-4}x + 0.02935$	0.99374	5–6,250	2.9	3.0
6	Isovaleric acid	3.0	5.0	$y = 2.07072e^{-4}x - 0.00303$	0.99654	5–12,500	2.1	3.5
7	2-Methylbutyric acid	0.5	2.0	$y = 2.80818e^{-4}x + 0.04874$	0.99846	5–25,000	7.5	8.1
8	2-Methylvaleric acid	3.0	5.0	$y = 9.89105e^{-5}x + 0.01038$	0.99559	10–12,500	2.2	8.7
9	3-Methylvaleric acid	2.0	5.0	$y = 4.94699e^{-5}x + 0.00142$	0.99892	5–6,250	3.2	5.5
10	4-Methylvaleric acid	0.5	1.5	$y = 1.54437e^{-4}x + 0.00749$	0.99805	2.5–6,250	6.4	5.2
11	Pivalic acid	0.5	2.0	$y = 2.78603e^{-4}x - 0.00476$	0.99929	5–6,250	5.0	3.1
12	2-Ethylbutyric acid	2.5	6.0	$y = 1.78141e^{-4}x - 0.03671$	0.99853	5–25,000	2.1	3.0
13	2,2-Dimethylbutyric acid	3.0	6.0	$y = 4.47025e^{-5}x - 0.01838$	0.99649	10–25,000	2.7	2.5
14	3,3-Dimethylbutyric acid	2.0	5.0	$y = 6.32423e^{-5}x - 0.00411$	0.99895	5–25,000	3.4	1.8
15	Hexanoic acid	1.0	3.0	$y = 1.99559e^{-4}x + 0.00403$	0.99917	5–6,250	6.2	1.2

y = area ratio of DMED/DEEA labeled SCFAs; x = concentration (nM).

Laboratories, Inc (CA). Valeric acid-d9 (C5:0-d9), hexanoic acid-d11 (C6:0-d11), and triglyceride (TG15:0-18:1-15:0) were purchased from Avanti Polar Lipids (AL). Charcoal-active granular material was obtained from Kelong Chemical (Chengdu, China). Dens-PP and Dens-HZ were synthesized in our laboratory as described in [supplemental data](#) ([supplemental Figs. S1–S4](#)). All other solvents and chemicals used were of analytical grade.

Biological samples

After fasting, the feces of 20 healthy volunteers (10 males, 10 females, average age of 50 ± 2 years) and 20 HCC individuals (10 males, 10 females, and average age of 50 ± 2 years) were collected. All subjects have been provided written consent in this study, and the protocol was approved by the local ethics committees (Army Medical University, Chongqing, China) and the procedures committees in accordance with the Declaration of Helsinki and Good Clinical Practice guidelines.

Analytical procedure

Stock and working solutions. Standard stock solutions of SCFAs, MCFAs, and LCFAs were prepared in ACN to obtain a concentration of 1 mM, respectively. The mixed standard working solutions of SCFAs were prepared with ACN via gradient dilution of stock solutions to obtain concentrations of 6.1, 12.2, 24.4, 48.8, 97.6, 195.3, 390.6, 781.2, 1562.5, 3125.0, 6250.0, 12500.0, and 25000.0 nM for calibrators. Similarly, quality control (QC) working solutions with 50.0, 500.0, and 5000.0 nM SCFAs were prepared as low, medium, and high solutions, respectively. Solutions of DMED, DEEA, CMPI, and TEA were prepared in ACN at the concentrations of 45.0, 45.0, 45.0, and 20.0 mM/ml, respectively. They were diluted with ACN to the desired levels before use. All stock and working solutions were freshly prepared.

Derivatization optimization. To optimize the reaction conditions, a stock mixture standard solution containing 1.0 μ M of the 15 types of SCFAs and a stock mixture containing 100.0 μ g/ml MCFAs and LCFAs were prepared in ACN and used as standards. Derivatization conditions were optimized in triplicates using different ratios of CMPI to DMED (1:1–1:8) and concentration of Dns-HZ (0.1–10.0 mg/ml) at 20–70°C for 20–180 min.

DMED/DEEA derivatization of SCFAs. The derivatization procedure is illustrated in [Fig. 1](#). Briefly, 30 μ l of a mixed standard solution containing 1.0 μ M of each SCFA was pipetted into a 10 ml glass tube. Then 15 μ l of 45.0 mM/ml CMPI solution, 30 μ l of 20.0 mM/ml TEA solution, and 200 μ l of ACN were added. After vortexing, the mixture was incubated at 50°C for 5 min, followed by adding 60 μ l of 45.0 mM/ml DMED or DEEA solution and vortexed for several seconds, and the mixture was incubated again at 50°C for 40 min. Next, the samples were dried under a constant flow of nitrogen using a 12-port drying manifold (Tri-I Biotech, Inc, Shanghai, China) and reconstituted with 200 μ l of ACN:H₂O (1:1, v/v). Finally, the sample was transferred to an autosampler vial containing a 300 μ l deactivated insert and centrifuged for 5 min at 10,000 rpm. The vial insert was then carefully transferred back to the autosampler vial and stored at –80°C until used for analysis. The DEEA-added solution was used as the DD-IS mix. Before analysis, the ratio of DD-ISs/analytes (1:1) was determined based on the identical concentrations.

Dns-HZ/Dens-HZ derivatization of MCFAs and LCFAs. The derivatization of MCFAs and LCFAs is shown in [Fig. 1](#). Briefly, 20 μ l of 100.0 μ g/ml mixed standard solution of MCFAs and LCFAs (C10:0–C24:0) was transferred into a 10 ml glass tube and dried under a constant flow of nitrogen. Then, 100 μ l of DCM, 2.5 μ l of *N,N*-dimethylformamide, and 20 μ l of oxalyl chloride (2 M in DCM) were sequentially added to the tube and vortexed for seconds. The reaction mixture was incubated for 0.5 h at 40°C and dried with nitrogen. Then, 20 μ l of Dns-HZ or Dens-HZ (5.0 mg/ml in ACN), 30 μ l of TEA (20.0 μ M/ml), and 100 μ l of DCM were added into the reactive system and incubated for 1.5 h. Finally, the mixture was dried up and reconstituted with 200 μ l of ACN.

Extraction of metabolites from fecal samples

Human fecal samples were homogenized as previously described (18). In brief, the fecal samples were homogenized in a gentle MACS™ Dissociator (Miltenyi Biotec GmbH, Bergisch Gladbach, Germany) in 70% IPA. The dry weight was determined by the overnight drying of an aliquot in a vacuum centrifuge. The fecal homogenates were diluted to a concentration of 2.0 mg dry weight/milliliter. The samples were stored at –80°C and kept on ice during processing. An aliquot of the homogenates was centrifuged, and the clear supernatant was subjected to DMED derivatization.

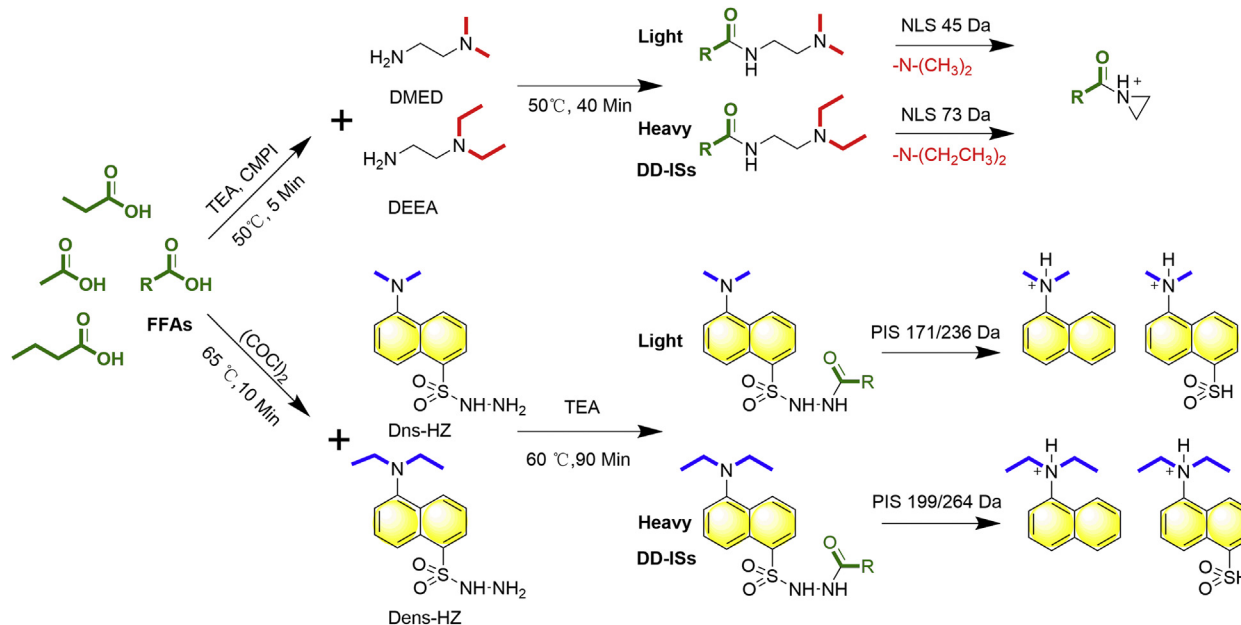


Fig. 1. The schematic graph for dual derivatization of FFAs using DMED/DEEA or Dns-HZ/Dens-HZ.

UPLC-MS/MS analysis

Using the Acquity UPLC system (Waters Corporation, Milford, MA), reversed phase separation was performed on an Acquity UPLC BEH C8 column (2.1 × 100 mm; 1.7 μm; Waters Corporation). The mobile phase consisted of ACN (A) and H₂O (B). The linear gradient conditions for the SCFAs were as follows: 0–2.0 min, 8% A; 2.0–6.0 min, 8–22% A; 6.0–7.0 min, 22–90% A; 7.0–7.1 min, 90–8% A; 7.1–8.0 min, 8% A, whereas the flow rate was set at 0.2 ml/min. The conditions for MCFAs and LCFAs were as follows: 0–1.0 min, 55% A; 1.0–9.0 min, 55–78% A; 9.0–12.0 min, 78% A; 12.0–15.0 min, 78–95% A; 15.0–17.0 min, 95% A; 17.0–18.0 min, 95–55% A; and 18.0–20.0 min, 55% A, whereas the flow rate was set at 0.4 ml/min. A 2 μl aliquot of each sample was injected into the column, and the column temperature was maintained at 40°C. All samples were kept at 4°C in sample trays throughout the analysis. MS was performed using an AB/SCIEX QTRAP 6500 spectrometer (Applied Biosystems, Foster City, CA). The FFA derivatives were detected in the positive electrospray ionization (+ESI) mode. Curtain gas (CUR), nebulizer gas (GSI), and turbo gas (GS2) were set at 25, 50, and 40 psi, respectively. The temperature of the turbo ion spray source was 400°C. The FFAs were analyzed using MRM. Mass spectrometer parameters including the declustering potential, entrance potential, collision energy, and collision cell exit potential were optimized for each analyte. Nitrogen was used as the collision gas. Data acquisitions were performed using Analyst 1.6.3 software (Applied Biosystems). MultiQuant software 3.0.2 (AB SCIEX) was used to quantify all the metabolites.

Data processing and quantification

All chemical structures in **Fig. 1** and **supplemental Figs. S1–S4** were drawn using ChemoBioDraw Ultra 14.0. OriginLab 2019b was used for **Figs. 2–4** as well as **supplemental Figs. S5–S11** and **S13**. Statistical analyses were performed using a two-tailed unpaired Student's *t*-test in GraphPad Prism 9.0.0 (GraphPad Software, La Jolla, CA). *P* values (***P* < 0.001, **P* < 0.01, and **P* < 0.05) were autolabeled

in **Fig. 5**. Statistical significance was set at *P* < 0.05. MetaboAnalyst 5.0 (<https://www.metaboanalyst.ca/>) was used for **Fig. 6** and **supplemental Fig. S12**.

Analytical validation

Linearity and sensitivity. Calibration was conducted based on the analysis of the derivatized SCFA standard working solutions. Calibration curves were established by employing a linear regression with a weighting factor of 1/*x*². The limit of detection (LOD) and limit of quantification (LOQ), estimated at signal-to-noise ratios near or above 3 and 10, respectively, were determined in five replicates for each SCFA.

Precision and accuracy. Intra-assay and interassay precision and accuracy were assessed by analyzing QC standards at three different levels. The intra-assay accuracy and precision were estimated using the recovery and coefficient of variation (CV) of the selected QC concentrations (*n* = 5), respectively. Interassay accuracy and precision were determined on three consecutive days (*n* = 15).

Stability. To determine the stability of the method, processed samples were stored at –80°C, then kept at 4°C in the autosampler, and injected for three times at 0, 1, 2, 3, and 4 weeks with the QC samples. The peak areas of the analytes were used to determine their stability at the subsequent time points.

Extraction efficiency. The extraction efficiency was determined by the recovery rate. Recovery rates were assessed by spiking a cocktail of C2:0-¹³C₂, C3:0-d₅, C4:0-d₇, C5:0-d₉, and C6:0-d₁₁ with low (50.0 nM), medium (500.0 nM), and high concentrations (5000.0 nM) into three aliquots of fecal extracts and standard solution ACN, respectively. The samples were then extracted and chemically labeled with DEEA for MS detection, and recovery rates were assessed by comparing the signal responses of the derivatized isotopes of SCFAs in fecal extracts to that of ACN.

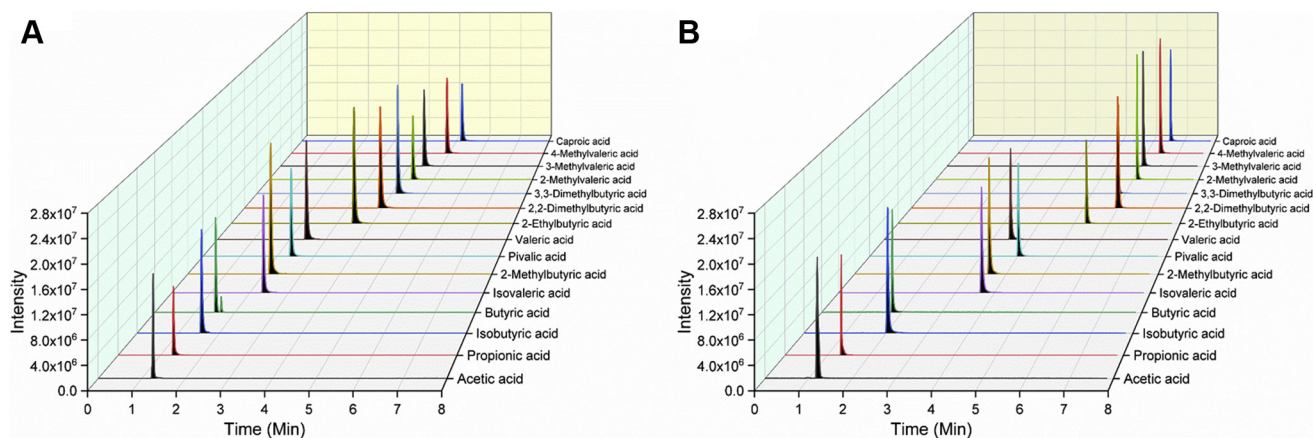


Fig. 2. Chromatograms of derivatized SCFAs by DMED/DEEA. DMED-SCFAs (A) and DEEA-SCFAs (B).

Matrix effect

Because of the lack of a truly SCFA-free matrix, we generated biologically blank feces homogenate by absorbing activated charcoal granules according to a previously reported method (19, 20). In brief, pooled feces samples (1.0 g) were dissolved in 10.0 ml of 70% IPA. Activated charcoal granules (0.5 g) were mixed into the solution, and the pH was adjusted to 3.0 by using 0.2 N of HCl. The mixture was then placed on ice and magnetically mixed for 1 h. Charcoal was then removed by centrifugation at 12,000 rpm at 4°C for

20 min in a Sorvall Legend Micro 21R centrifuge (Thermo Fisher Scientific, MA). The clarified solution was then brought to pH 7.0 (Sartorius Basic PH Meter PB-10; Sartorius AG, Goettingen, Germany) by adding 0.2 N NaOH. The resulting solution was used as the blank feces homogenate and evaluated by DMED derivatization. QC standard working solutions with low, medium, and high concentrations were derivatized by DMED, respectively. The labeled solutions were then added to the aforementioned blank feces homogenate matrix and ACN to estimate the impact of the matrix

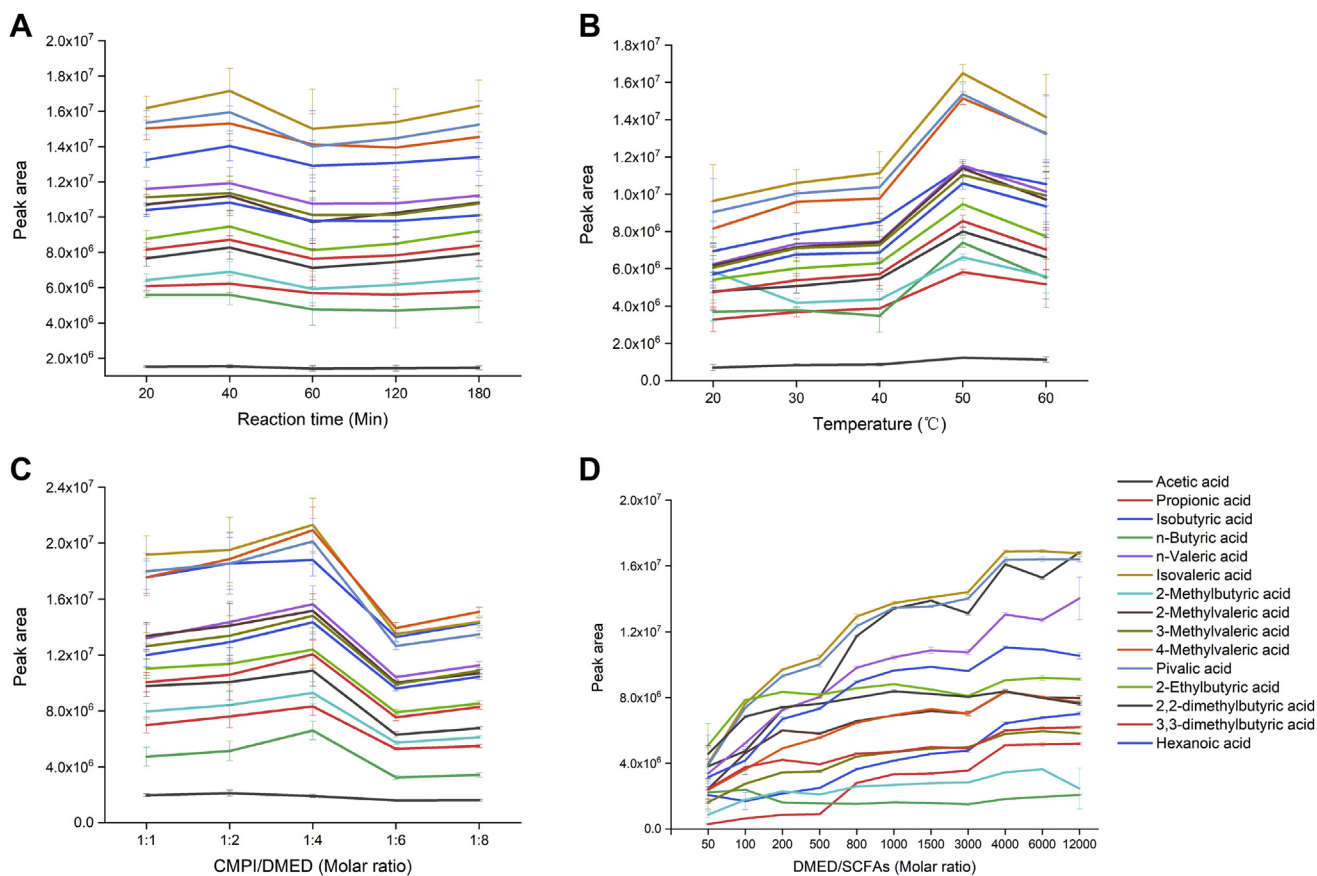


Fig. 3. Optimization of derivatization time (A), temperature (B), CMPI/DMED (C), and DMED/SCFA (D) on peak areas of formed SCFAs.

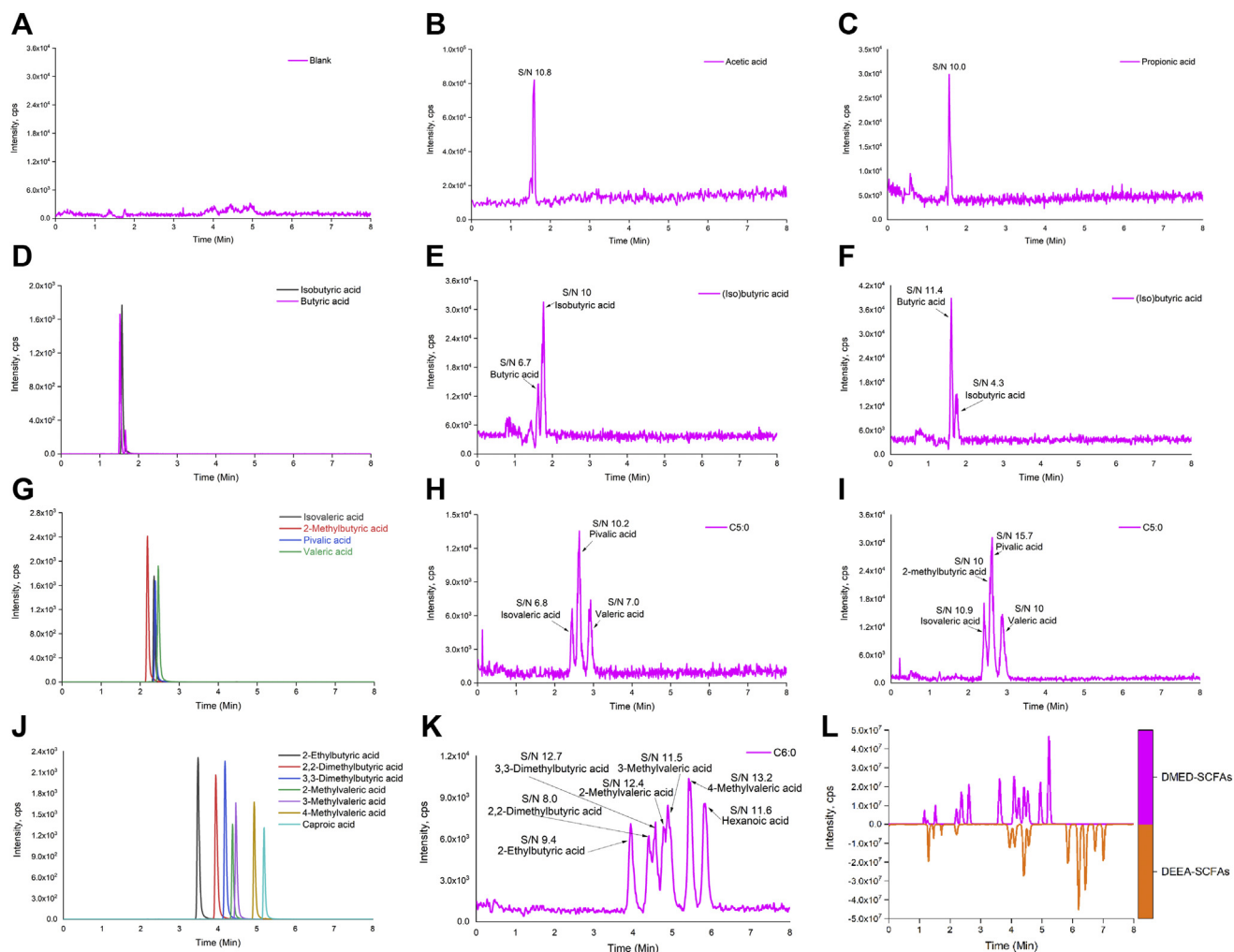


Fig. 4. The extracted ion and LOQ chromatography of indicated SCFAs and DMED/DEEA-SCFAs. Extracted ion chromatography of indicated SCFAs (A, D, G, and J). LOQ chromatography of indicated SCFAs (B, C, E, F, H, I, and K). Total ion chromatography of DMED/DEEA-SCFAs (L).

components. The matrix effect was assessed by the ratio of the DMED-SCFAs signal in the feces matrix to that of ACN.

To further assess the derivatization yield discrepancy in the feces homogenates and ACN, QC samples in both matrices were derivatized with DMED, and the yields were calculated by comparing the ratio of the peak areas in the two different matrices. All determinations were performed in triplicates.

RESULTS

Labeling optimization

To develop a method that combines isotope-free method with dual derivatization and UPLC-MS/MS MRM method for the sensitive and comprehensive quantification of FFAs, a pool of commercially available and well-designed derivatization reagents, namely DMED and its analogue DEEA, Dns-Hz and its analogue Dens-HZ, were utilized, based on either the primary amine moiety possessing excellent reactivity toward carboxyl groups or the readily protonated tertiary amine scaffolds in the positive ESI mode (Fig. 1).

Molecules coupled with the aforementioned entities facilitated the polarity tuning and chromatographic retention compared with the other underivatized components, thereby enhancing the resolution of chromatography and eliminating the competition for ionization (Fig. 2 and supplemental Fig. S5). In addition, the amplified signal from the charged tertiary amine group substantially boosted the sensitivity. DMED/DEEA for SCFA derivatization prolonged the reaction time to 180 min, which failed to further intensify the peak area of each analyte; thus, 40 min was selected for the reaction (Fig. 3A). As the temperature increased, the peak intensity increased. However, a decrease in the peaks for almost every compound was observed at 60°C. Therefore, 50°C was chosen for the subsequent reactions (Fig. 3B). Moreover, the molar ratio of CMPI to DMED at 1:4 showed the most effective derivatization (Fig. 3C), whereas the plateau phase of the signal with the DMED/SCFA ratio was reachable until 4,000 (Fig. 3D). Hence, the optimal conditions for DMED/DEEA derivatization were set to 50°C, 40 min

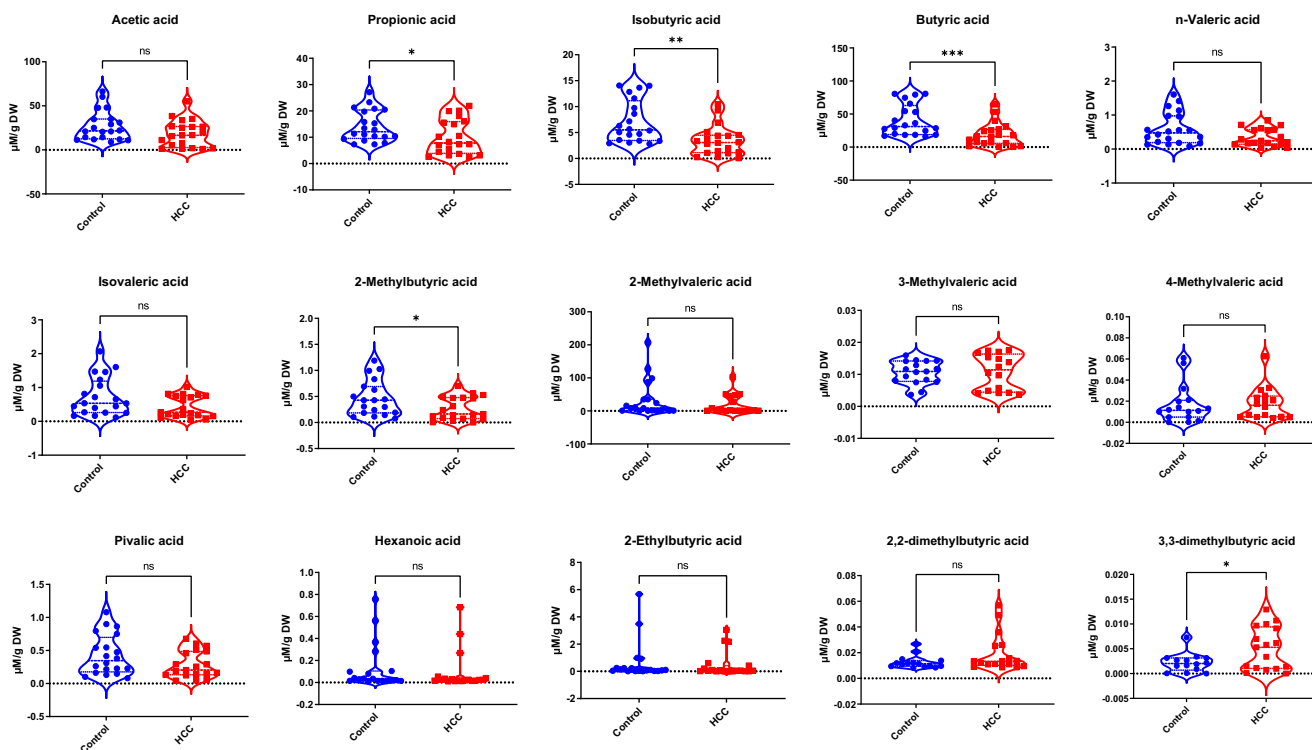


Fig. 5. The concentration of SCFAs determined in fecal samples of healthy controls versus HCC patients.

incubation with a molar ratio of CMPI/DMED at 1:4, and DMED/SCFA under 4,000. Similar optimal reaction conditions including temperature (60°C), reaction time (90 min), substrate concentration (Dns-HZ 2.5 mg/ml), and solvent (TCM) for the Dns-HZ/Dens-HZ system were optimized and displayed in [supplemental Figs. S6–S8](#).

Strategy of DD-ISs

Owing to the structural similarity and diversity of FFAs, a one-to-one IS was ideally required to precisely quantify compounds of interest. However, it is extremely difficult to synthesize a wide range of stable isotope-labeled IS. Therefore, we implemented a strategy that integrated isotope-free method with dual derivatization using DMED/DEEA (or Dns-HZ/Dens-HZ) as an alternative, in which DEEA (or Dens-HZ)-derivatized FFA standards were utilized as DD-ISs of the DMED (or Dns-HZ)-derivatized samples ([Fig. 1](#)). Notably, this method exhibited high efficiency, robustness, and consistency with respect to FFA detection. Concurrently, it generated one-to-one DD-ISs with constant mass defects and substantial retention time shifts.

UPLC-MS/MS analysis

The derivatives harbored a constant neutral loss scan of 45 Da for DMED-SCFAs and 73 Da for DEEA-SCFAs by eliminating the dimethylamine (DMED) or diethylamine (DEEA) neutral fragments of the amine C-N bond, indicating the MRM transition ([Fig. 1](#) and [Table 1](#)).

Subsequently, each parameter for mass detection of SCFAs was optimized as listed in [Table 1](#). In addition, the reverse phase LC gradient elution program for the separation of SCFAs along with FFAs was meticulously tuned. Representative extracted ion chromatograms acquired from a mixed standard solution of SCFAs after derivatization are also shown in [Fig. 2](#) and [supplemental Fig. S5](#). Consequently, every single analyte and its corresponding DD-IS obtained the optimal resolution. The identical MRM parameters for the Dns-HZ/Dens-HZ and Dns-PP/Dens-PP system are provided in [supplemental Tables SI–S4](#), and precursor ion scan was used to construct the MRM ion pairs.

Method validation

A series of experiments including linearity, calibration range, accuracy, precision, stability, extraction efficacy, matrix effect, and specificity for SCFA quantification validated the proposed DMED/DEEA method under optimized conditions. As shown in [Table 2](#), satisfactory correlation coefficients were obtained ranging from 0.99374 to 0.99929, and the LODs and LOQs for SCFAs were within the range of 0.5–3 and 1.5–6 nM, respectively ([Fig. 4](#)). The detection sensitivities of DMED-labeled SCFAs were remarkably higher in the positive ESI (+ESI) mode than in the full scans of intact SCFAs in the negative ESI (–ESI) mode. The accuracy and precision were evaluated by the three-level QC standards' intra-assay and interassay performance of the three-level QC standards, which were higher than 80%, whereas isobutyrate gained 68%

during the intra-assay at 5,000 nM (supplemental Table S5). Furthermore, in the chromatography peaks, the high concentration tagging failed to feasibly separate isobutyrate from its isomer butyrate. The stability of the derivatives is shown in supplemental Fig. S9A, which illustrates that the samples could be stored at -80°C for at least 3 weeks. The extraction efficiencies varied from 83.7% to 105.0%, demonstrating the acceptable purification effect of the proposed method (supplemental Fig. S9B and supplemental Table S6).

To evaluate the matrix effect of our established method, the biologically blank feces homogenate was labeled by DMED to approve the absorption efficiency using active charcoal, as illustrated in supplemental Fig. S9C, and no apparent SCFA residue existed. Based on the blank homogenate and ACN, the matrix effects measured ranged from 82.70% to 113.3% (supplemental Table S7), indicating a slight matrix effect and good reproducibility (CV% 3.5–13.3). The derivatization yields in the feces homogenate and ACN were also evaluated, which fluctuated from 79.9% to 108.3% with CV% of 2.4–12.7. Thus, there was no noticeable interference from the complex matrix of feces.

The interference of fatty acyl moieties of lipids was consequently verified. TG15:0-18:1-15:0 was added as a substrate into the reaction system, and no significant peaks of 15:0 and 18:1 fatty acyl products after derivatization were observed (supplemental Fig. S9D). Likewise, hybrid signals from reaction additives were excluded because of a lack of DMED/DEEA among the reaction mixture (supplemental Fig. S10A). Furthermore, this method also showed a signal intensity that was two or three magnitudes higher than that of the signal intensity when compared with straightforward LC-MS analysis of intact SCFAs by using the negative MRM mode with the equal precursor (Q1) and daughter ion (Q3) (supplemental Fig. S10B). Excellent chromatographic resolution and characteristic fragments of DMED/DEEA-SCFAs derivatives were also simultaneously achieved. These enhanced signals further improved the assay validity of the method with lower LOD, LOQ, and a better linear range as previously described (21–24).

Method application

Aberrant metabolism correlates with biochemical and clinical consequences, and the precise quantitation of SCFAs provides preliminary evidence of these discrepancies. SCFAs can be produced by gut fermentation of soluble fibers from food components, which are generally considered health promoting. For example, propionate, butyrate, and isobutyrate are generated by a set of gut bacteria, such as *Roseburia*, *Faecalibacterium Oscillospira spp.*, *Prevotella*, *Bacteroides*, and *Fusobacterium* (25). The 16S rRNA gene sequencing systematically can characterize the decaying abundance of these linked bacteria (26). Accordingly, the consumption of such

fibers ameliorates the metabolic syndrome. However, dietary soluble fibers (e.g., inulin) may induce cholestasis and HCC (27). Determining the SCFAs in the feces of patients with HCC may provide potential biomarkers for diagnosis and prognosis.

Employing the previously established method, we measured the levels of SCFAs in fecal samples of 20 HCC patients and 20 healthy individuals and found that the total amount of SCFAs was lower in HCC patients than in healthy controls. A notable decrease was observed in the propionate, butyrate, isobutyrate, and 2-methylbutyrate in the HCC fecal samples. In contrast, 3,3-dimethylbutyric acid significantly increased, which might be a product of butyric acid. Acetate, methylvaleric acid, valeric acid, isovaleric acid, pivalic acid, and hexanoic acid were comparable between the two groups (Fig. 5, supplemental Fig. S11, and supplemental Table S8). On further annotation of these data with MetaboAnalyst 5.0, the orthogonal partial least-squares discrimination analysis indicated that SCFA metabolic heterogeneity occurred because there was a cross-section between HCC patients and normal individuals (Fig. 6A). Metabolic variation could be responsible for the result as clustering analysis showed differences in acetate, propionate, and (iso)butyrate (cluster 1: normal—6, 11, 15, 17, etc.) or 2-methylbutyrate, pivalic acid, and (iso)valeric acid (cluster 2: HCC—4, 8, 12, 18, etc.) or both (cluster 3: HCC—7, 9, 11, 19, etc.). Thus, the heatmap featured the main clusters of these samples (Fig. 6B and supplemental Fig. S12).

MCFAs and LCFAs were also tentatively tested in the DMED/DEEA system. Owing to challenges such as the low ionization response and dynamic ranges of FFAs, a one-fit-all method for simultaneously monitoring different FFAs is yet to be developed. We extended our established method to measure C10:0 to C24:0. This attempt gained consistent high fidelity from MCFAs to LCFAs with an elongated LC time (supplemental Figs. S10C, D). This explicated the potential application of this method in the quantification of a broad coverage of FFAs.

DISCUSSION

In this study, an analytical method that integrated isotope-free and the dual derivatization LC-MS MRM strategies was successfully established and validated for the simultaneous separation and quantitation of 15 types of C2–C6 SCFAs in human fecal samples as well as MCFAs and LCFAs in standard mixtures. The application of DMED/DEEA (or Dns-HZ/Dens-HZ) derivatization has several advantages over other derivatization methods, as well as the LC-MS straightforward analysis of intact FFAs (supplemental Fig. S10B). The reaction under the optimized conditions exhibited excellent in-solution stability, which was especially useful for high-throughput sample analysis and patient-oriented sampling as therapeutic processes are

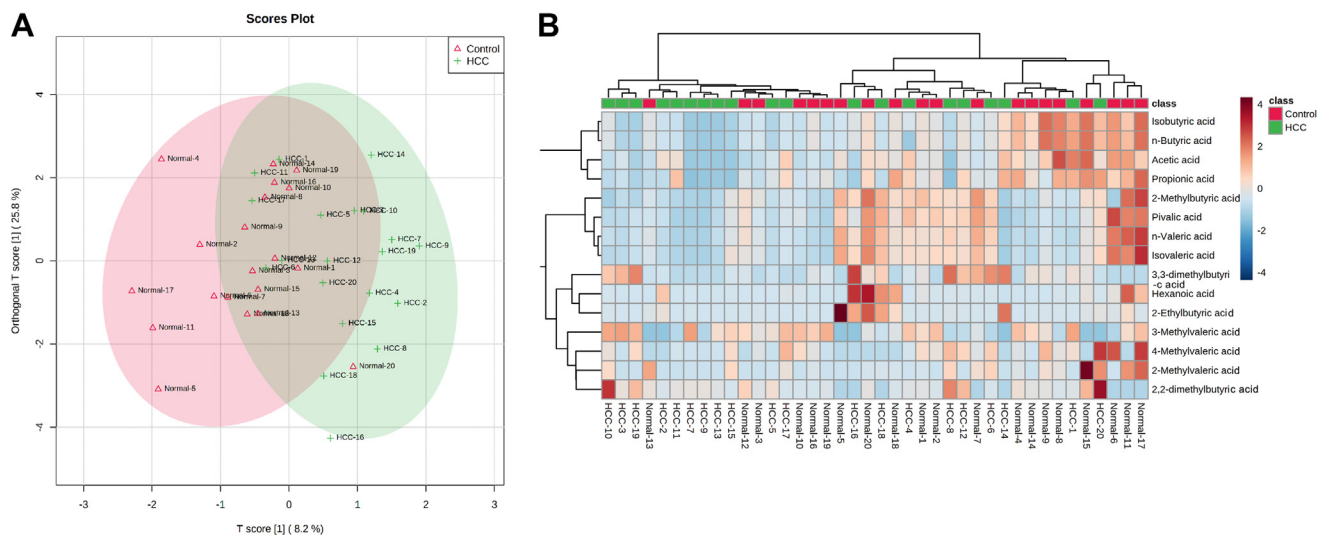


Fig. 6. OPLS-DA and clustering analysis of SCFAs in fecal samples of healthy controls versus HCC patients. OPLS-DA of SCFAs (A). Clustering analysis of SCFAs (B). OPLS-DA, orthogonal partial least-squares discrimination analysis.

not always streamed. Thus, in-solution stability thus confers long-term sample storage. Compared with other CD approaches, no quenching procedure is required, which further simplifies the preprocessing. Moreover, DMED/DEEA showed no significant substrate interference, as excessive reaction substrates were volatile and could be easily eliminated under a constant nitrogen stream. A mixture of stable DEEA (or Dens-HZ)-labeled DD-ISs could also be individually assigned to every analyte. In addition, the DMED/DEEA system could be extended to a broad coverage of C8–C24 via fine-tuned reaction conditions with prolonged LC runtime as Dns-HZ/Dens-HZ system (supplemental Figs. S10C, D).

Admittedly, dansyl hydrazine is typically used in the derivatization of aldehyde/ketones because of its carbonyl moiety. Recent studies have also demonstrated its potential in carboxylic acid submetabolome profiling (16). Mechanistically, the hydrazide group in Dns-Hz can be linked to carboxylic acids using a coupling reagent, namely 1-ethyl-3-(3-dimethylaminopropyl) carbodiimide, whereas 1-hydroxy-7-azabenzotriazole can be simultaneously utilized as a catalyst under acidic conditions (MES buffer pH 3.5). However, we were unable to achieve robust derivatized products every single time using the same reagents despite the relatively mild reaction conditions. Alternatively, we used oxalyl chloride for preparing acylamide. A previous study showed that oxalyl chloride and 3-picolylamine were superior to dimethylaminoethyl ester and 3-picolinyl ester. Thus, the combination of oxalyl chloride and 3-picolylamine was accordingly developed to determine FFAs in red blood cells (28). Hence, these studies inspired us to use oxalyl chloride in our Dns-HZ/Dens-HZ system. By labeling optimization, the temperature (60°C), reaction time (90 min), substrate concentration (Dns-HZ 2.5 mg/ml), and solvent (TCM) were optimized (supplemental

Figs. S6–S8). A constant precursor ion scan further verified the derivatization regime. Moreover, oxalyl chloride, as a labile chemical, can react water in the atmosphere and abort the reaction. Therefore, a sufficient amount of MgSO_4 (50.0 mg) was added to the test tube to ensure a dry atmosphere. Such a combination of desiccant and temperature was sufficient to transfer FFAs into acyl chloride during organic synthesis. Our results further confirmed the robustness and sensibility of Dns-HZ/Dens-HZ derivatization by means of oxalyl chloride.

Nonetheless, the limitation of this method is that the isotope-free method with dual derivatization strategy did not fully address the sample extraction efficiency with respect to account for sample-to-sample variation (diet, etc.). Thus, we added low, medium, and high concentrations of isotopic standards to the sample mixture prior to extraction to measure in sample recoveries. This was also a trade-off strategy with regard to larger numbers of metabolites where fewer labeled ISs could be extrapolated across all other for evaluating the extraction efficiency (supplemental Fig. S9B and supplemental Table S6). Furthermore, we could not disregard the impact of the mobile phase additives, such as acetic acid, on the detection of acetate owing to in-column derivatization. Since peak interference was present in this scenario, while using formic acid could be an acceptable alternative. Similarly, Xu *et al.* exploited this strategy using Dns-PP/Dens-PP quantitative profiling of eicosanoids derived from n-6 and n-3 polyunsaturated FAs, FFAs, and multiple chemical group-based submetabolomes (17, 29, 30). These methods not only improved the LC separation of the targets but also enhanced the ion MS response.

To further validate that our proposed method could be successfully applied to determine the absolute/relative content of metabolites, we synthesized Dens-PP


(supplemental Figs. S1, S4) and exploited Dns-PP/Dens-PP to derivatize FFAs. As shown in supplemental Figs. S13 and supplemental Tables S3–S4, Dns-PP/Dens-PP showed excellent labeling sensitivity toward FFAs. Conversely, the labeling efficiency was attenuated with increased aliphatic chains in the iso-concentration of the FFA mixture. This diminished derivatization efficiency was also observed in the Dns-HZ/Dens-HZ system (supplemental Fig. S7). In contrast, the steric hindrance effect of the amine moiety of hydrazine was weaker than that of the piperazinyl group. Thus, the Dns-HZ/Dens-HZ system exhibited a more enhanced derivatization efficiency for quantifying the MCFA and LCFA carboxylic acid submetabolome (supplemental Fig. S7). In addition, SCFAs are volatile, and dried samples generated through nitrogen flow are needed for Dns-HZ labeling. Therefore, Dns-PP and DMED were much more feasible for SCFA derivatization.

FFAs play diverse roles in diseases, which prompted us to further quantify the fluctuation of SCFAs in HCC. It is a gastroenterological disease where microbiome-fermented SCFAs flow through the portal vein entering the liver, exposing the tumor microenvironment (4, 25). These invisible gut-liver-microbiome triads are deeply rooted in the HCC through metabolite transformation and energy circulation (2). Among these, acetate, propionate, and butyrate are strong indicators of metabolic reprogramming in macrophage function, orchestrated disease severity, and prognosis (8). Our proposed method efficiently quantified diminished propionate, butyrate, isobutyrate, and 2-methylbutyrate in the feces of patients with HCC. Further normalization of the data by using MetaboAnalyst 5.0 (supplemental Fig. S12A) suggested that the attenuated trends of propionate, butyrate, and isobutyrate were positively correlated with each other. In contrast, the negative correlation of 2-methylbutyrate with those following decreased metabolites was seen in supplemental Fig. S12B, which might be attributed to a salvage synthesis pathway from isoleucine. The readily interchangeable pathways among acetate, butyrate, and isobutyrate are well known. However, propionate, as the main product of the microbiome, dynamically interacts with these physiologically active molecules. In this study, we could not provide a suitable mechanistic explanation of the discrepancy, but these reduced trends are consistent with decayed microbiota during HCC progression (1, 26, 27). Therefore, it seems promising to prescribe prebiotics or probiotics to HCC patients with dysfunctional microbiota.

This work provides an easy-to-use and comprehensive strategy for quantifying of FFAs, in addition to quantifying these metabolites in the feces of HCC patients. Broad coverage of the derivatization method showed excellent sensitivity and specificity. Furthermore, the dual derivatization of the ISs made it possible for individual quantification. This strategy could be

adapted to trace FFA levels in biosamples as it might yield potential biomarkers for independent and noninvasive diagnosis protocols.

Data availability

All data supporting this study are included in the article and supplemental data. 

Supplemental data

This article contains supplemental data.

Author contributions

J. Z., S. Y., Yan Li, and Yongsheng Li conceptualization; J. Z., S. Y., Yan Li, and Yongsheng Li methodology; J. Z., S. Y., H. Z., J. L., Y. Z., L. W., Yan Li, and Yongsheng Li software; Y. Z., J. L., H. Z., and L. W. validation; J. W., Y. X., and M. Z. investigation; J. Z. and S. Y. data curation; J. Z. and S. Y. writing—original draft; Yongsheng Li writing—review and editing; J. W., Y. X., and M. Z. visualization; Yan Li and Yongsheng Li supervision.

Funding and additional information

This work was supported by the Major International (Regional) Joint Research Program of the National Natural Science Foundation of China (grant no. 81920108027 to Yongsheng Li), Chongqing Outstanding Youth Science Foundation (grant no. cstc2020jcyj-jqX0030 to Yongsheng Li), and funding for University Innovation Research Group of Chongqing (to Yongsheng Li), and Chongqing Municipal Science Technology Commission (grant no. cstc2018jcyj-AX0185 to Yan Li).

Conflict of interest

The authors declare that they have no conflicts of interest with the contents of this article.

Abbreviations

ACN, acetonitrile; CD, chemical derivatization; CMPI, 2-chloro-1-methylpyridinium iodide; CV, coefficient of variation; DCM, dichloromethane; DD-IS, dual derivatization internal standard; DEEA, *N,N*-diethyl ethylene diamine; Dens-HZ, *N,N*-diethyldansulfonyl hydrazide; Dens-PP, diethylamino-naphthalene-1-sulfonyl piperazine; DMED, 2-dimethylaminoethylamine; Dns-Hz, dansyl hydrazine; Dns-PP, 5-dimethylamino-naphthalene-1-sulfonyl piperazine; ESI, electrospray ionization; HCC, hepatocellular carcinoma; IPA, isopropanol; LCFA, long-chain FA; LOD, limit of detection; LOQ, limit of quantification; MCFA, medium-chain FA; MRM, multiple reaction monitoring; QC, quality control; SCFA, short-chain FA; TCM, trichloromethane; TEA, triethylamine.

Manuscript received August 18, 2021, and in revised form October 17, 2021. Published, JLR Papers in Press, October 26, 2021, <https://doi.org/10.1016/j.jlr.2021.100143>

REFERENCES

1. Currie, E., Schulze, A., Zechner, R., Walther, T. C., and Farese, R. V., Jr. (2013) Cellular fatty acid metabolism and cancer. *Cell Metab.* 18, 153–161

2. Kimura, I., Ichimura, A., Ohue-Kitano, R., and Igarashi, M. (2020) Free fatty acid receptors in health and disease. *Physiol. Rev.* **100**, 171–210
3. Cahill, G. F., Jr. (2006) Fuel metabolism in starvation. *Annu. Rev. Nutr.* **26**, 1–22
4. Alvarez-Curto, E., and Milligan, G. (2016) Metabolism meets immunity: The role of free fatty acid receptors in the immune system. *Biochem. Pharmacol.* **114**, 3–13
5. Sivaprakasam, S., Prasad, P. D., and Singh, N. (2016) Benefits of short-chain fatty acids and their receptors in inflammation and carcinogenesis. *Pharmacol. Ther.* **164**, 144–151
6. Burdge, G. C., and Lillycrop, K. A. (2014) Fatty acids and epigenetics. *Curr. Opin. Clin. Nutr. Metab. Care.* **17**, 156–161
7. Sabari, B. R., Zhang, D., Allis, C. D., and Zhao, Y. (2017) Metabolic regulation of gene expression through histone acylations. *Nat. Rev. Mol. Cell Biol.* **18**, 90–101
8. O'Keefe, S. J. (2016) Diet, microorganisms and their metabolites, and colon cancer. *Nat. Rev. Gastroenterol. Hepatol.* **13**, 691–706
9. Chiu, H. H., and Kuo, C. H. (2020) Gas chromatography-mass spectrometry-based analytical strategies for fatty acid analysis in biological samples. *J. Food Drug Anal.* **28**, 60–73
10. Tumanov, S., Bulusu, V., and Kamphorst, J. J. (2015) Analysis of fatty acid metabolism using stable isotope tracers and mass spectrometry. *Methods Enzymol.* **561**, 197–217
11. Gelpi, E. (1995) Biomedical and biochemical applications of liquid chromatography-mass spectrometry. *J. Chromatogr. A.* **703**, 59–80
12. Kortz, L., Dorow, J., and Ceglarek, U. (2014) Liquid chromatography-tandem mass spectrometry for the analysis of eicosanoids and related lipids in human biological matrices: A review. *J. Chromatogr. B Analyt. Technol. Biomed. Life Sci.* **964**, 1–11
13. Han, J., Lin, K., Sequeira, C., and Borchers, C. H. (2015) An isotope-labeled chemical derivatization method for the quantitation of short-chain fatty acids in human feces by liquid chromatography-tandem mass spectrometry. *Anal. Chim. Acta.* **854**, 86–94
14. Chan, J. C., Kioh, D. Y., Yap, G. C., Lee, B. W., and Chan, E. C. (2017) A novel LCMSMS method for quantitative measurement of short-chain fatty acids in human stool derivatized with ¹²C- and ¹³C-labelled aniline. *J. Pharm. Biomed. Anal.* **138**, 43–53
15. Zhu, Q. F., Hao, Y. H., Liu, M. Z., Yue, J., Ni, J., Yuan, B. F., and Feng, Y. Q. (2015) Analysis of cytochrome P450 metabolites of arachidonic acid by stable isotope probe labeling coupled with ultra high-performance liquid chromatography/mass spectrometry. *J. Chromatogr. A.* **1410**, 154–163
16. Zhao, S., and Li, L. (2018) Dansylhydrazine isotope labeling LC-MS for comprehensive carboxylic acid submetabolome profiling. *Anal. Chem.* **90**, 13514–13522
17. Jiang, R., Jiao, Y., Zhang, P., Liu, Y., Wang, X., Huang, Y., Zhang, Z., and Xu, F. (2017) Twin derivatization strategy for high-coverage quantification of free fatty acids by liquid chromatography-tandem mass spectrometry. *Anal. Chem.* **89**, 12223–12230
18. Liebisch, G., Ecker, J., Roth, S., Schweizer, S., Öttl, V., Schött, H. F., Yoon, H., Haller, D., Holler, E., Burkhardt, R., and Matysik, S. (2019) Quantification of fecal short chain fatty acids by liquid chromatography tandem mass spectrometry-investigation of pre-analytical stability. *Biomolecules.* **9**, 121
19. Chen, R. F. (1967) Removal of fatty acids from serum albumin by charcoal treatment. *J. Biol. Chem.* **242**, 173–181
20. Carter, P. (1978) Preparation of ligand-free human serum for radioimmunoassay by adsorption on activated charcoal. *Clin. Chem.* **24**, 362–364
21. Dei Cas, M., Paroni, R., Saccardo, A., Casagni, E., Arnoldi, S., Gambaro, V., Saresella, M., Mario, C., La Rosa, F., Marventano, I., Piancone, F., and Roda, G. (2020) A straightforward LC-MS/MS analysis to study serum profile of short and medium chain fatty acids. *J. Chromatogr. B Analyt. Technol. Biomed. Life Sci.* **1154**, 121982
22. Nagatomo, R., Okada, Y., Ichimura, M., Tsuneyama, K., and Inoue, K. (2018) Application of 2-picolylamine derivatized ultra-high performance liquid chromatography tandem mass spectrometry for the determination of short-chain fatty acids in feces samples. *Anal. Sci.* **34**, 1031–1036
23. Chen, L., Sun, X., Khalsa, A. S., Bailey, M. T., Kelleher, K., Spees, C., and Zhu, J. (2021) Accurate and reliable quantitation of short chain fatty acids from human feces by ultra high-performance liquid chromatography-high resolution mass spectrometry (UPLC-HRMS). *J. Pharm. Biomed. Anal.* **200**, 114066
24. Fu, H., Zhang, Q. L., Huang, X. W., Ma, Z. H., Zheng, X. L., Li, S. L., Duan, H. N., Sun, X. C., Lin, F. F., Zhao, L. J., Teng, G. S., and Liu, J. (2020) A rapid and convenient derivatization method for quantitation of short-chain fatty acids in human feces by ultra-performance liquid chromatography/tandem mass spectrometry. *Rapid Commun. Mass Spectrom.* **34**, e8730
25. Morrison, D. J., and Preston, T. (2016) Formation of short chain fatty acids by the gut microbiota and their impact on human metabolism. *Gut Microbes.* **7**, 189–200
26. Huang, H., Ren, Z., Gao, X., Hu, X., Zhou, Y., Jiang, J., Lu, H., Yin, S., Ji, J., Zhou, L., and Zheng, S. (2020) Integrated analysis of microbiome and host transcriptome reveals correlations between gut microbiota and clinical outcomes in HBV-related hepatocellular carcinoma. *Genome Med.* **12**, 102
27. Singh, V., Yeoh, B. S., Chassaing, B., Xiao, X., Saha, P., Aguilera Olvera, R., Lapek, J. D., Jr., Zhang, L., Wang, W. B., Hao, S., Flythe, M. D., Gonzalez, D. J., Cani, P. D., Conejo-Garcia, J. R., Xiong, N., et al. (2018) Dysregulated microbial fermentation of soluble fiber induces cholestatic liver cancer. *Cell.* **175**, 679–694.e622
28. Li, X., and Franke, A. A. (2011) Improved LC-MS method for the determination of fatty acids in red blood cells by LC-orbitrap MS. *Anal. Chem.* **83**, 3192–3198
29. Huang, Y., Jiao, Y., Gao, Y., Zhang, P., Huang, W., Liu, Y., Huang, Y., Tian, Y., Wan, J. B., Zhang, Z., Hao, K., and Xu, F. (2019) An extendable all-in-one injection twin derivatization LC-MS/MS strategy for the absolute quantification of multiple chemical-group-based submetabolomes. *Anal. Chim. Acta.* **1063**, 99–109
30. Xia, F., He, C., Ren, M., Xu, F. G., and Wan, J. B. (2020) Quantitative profiling of eicosanoids derived from n-6 and n-3 polyunsaturated fatty acids by twin derivatization strategy combined with LC-MS/MS in patients with type 2 diabetes mellitus. *Anal. Chim. Acta.* **1120**, 24–35